

## PETROGRAPHY, CHEMISTRY AND NOBLE GAS COSMOCHEMISTRY OF NEBULA CONDENSATE

**DJERFISHERITE IN ENSTATITE CHONDRITES.** P.L. Clay<sup>1</sup>, H. Busemann<sup>1</sup>, A. El Goresy<sup>2</sup>, and R. Wieler<sup>3</sup>.

<sup>1</sup>SEAES, University of Manchester, Manchester M13 9PL, UK. (patricia.clay@manchester.ac.uk). <sup>2</sup>BGI, Universität Bayreuth, Germany. <sup>3</sup>ETH Zurich, Institute for Geochemistry and Petrology, 8092 Zurich, Switzerland.

**Introduction:** A precise chronology of the events in the early solar system is crucial for understanding its evolution from the collapse of the parent molecular cloud, through the formation of the first solid nebula condensates to the planetary bodies as present now. Numerous chronometers can be applied to date formation, differentiation, cooling and secondary thermal resets, e.g. by impact [1-3].

While short-lived chronometers date events in the first few tens of Ma with a high chronological resolution, they require calibration with a long-lived chronometer for absolute ages [4-5]. Minerals that can be dated simultaneously with multiple chronometers are most suitable. However, even when a single mineral hosts the parent nuclides of two chronometers, one chronometer may be more resistant to resetting and the systems may date different events; furthermore such minerals, where both, an appropriate long- and short-lived system can be applied, are rare [4,6].

In previous work, we have identified a mineral phase in which two hitherto unlinked chronometers can be simultaneously determined: the long-lived absolute Ar-Ar system and the short-lived, relative I-Xe system [7-9]. In-vacuo, Closed-System Step Etching experiments (CSSE [10]) with HF at ETH Zurich on a bulk sample of the E chondrite St. Mark's revealed the correlated release of radiogenic excess ( ${}^*\text{Ar}$ ) and  ${}^{129}\text{Xe}$  (Fig. 1 [7-9]). The strong correlation ( $r^2 > 0.99$ ) in the first 5 etch steps indicates a common carrier phase highly susceptible to HF. As K in St. Mark's is mostly partitioned with Fe and Cu in djerfisherite ( $\sim 10$  wt% K, [11,12]), the released radiogenic  ${}^*\text{Ar}$  and the correlated  ${}^{129}\text{Xe}$  originate most likely from this sulfide ( $\text{K,Na}_6(\text{Fe,Ni,Cu})_{25}\text{S}_{26}\text{Cl}$  [13]). The presence of the halogens Cl and Br (and hence probably also I [14]) in djerfisherite ( $\sim 1.5$  wt% Cl [11,12,15] and 170 ppm Br [16]), and the simultaneous release of cosmogenic Ne with low  ${}^{21}\text{Ne}/{}^{22}\text{Ne}$  [7-9], indicative of Na, identifies the host phase of these radiogenic components as djerfisherite (0.3-1.75 wt% Na [11,12,15]). This rare mineral, actually discovered in St. Mark's [17], occurs in mostly very small grains almost exclusively in E chondrites. The etch experiment revealed a second phase that is less susceptible to etching with HF and also shows a correlated release of  ${}^*\text{Ar}$  and  ${}^{129}\text{Xe}$  (not shown here), with a much higher initial I/K ratio, potentially pyroxene.

Online etching of irradiated djerfisherite will allow us to test the proposed absolute calibration of the I-Xe

chronometer by comparing absolute ages between this short-lived and the long-lived Ar-Ar system in primitive meteorites and it will help us to seek an explanation for the discrepancy between the Mn-Cr and I-Xe systems [18].

Moreover, djerfisherite will serve itself as a prime target for chronology of events during the E chondrite parent body evolution: (i) It is suggested to have formed by condensation in the nebula; E chondrites contain a variety of primary sulfides that are located as clasts and nodules in the Si matrix [12]. (ii) Djerfisherite is also easily susceptible to alteration, such as is observed with the "Qingzhen" break-down reaction into porous troilite (see also below), possibly in response to thermal metamorphism [15].

Here, we present initial petrographic and chemical analyses of djerfisherite grains that have been selected for extraction from two E chondrites for correlated I-Xe and Ar-Ar analysis, with a further subsection reserved for Rb-Sr analysis.

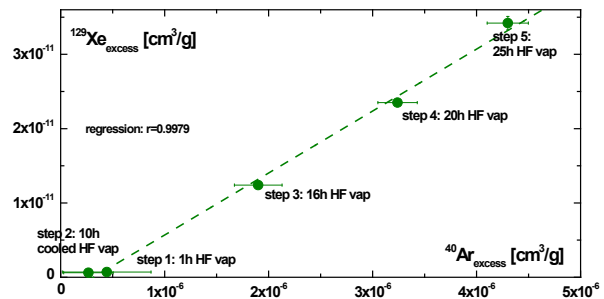


**Fig. 1** Radiogenic  ${}^{129}\text{Xe}$  and  ${}^*\text{Ar}$  in the first HF online etch steps of a bulk sample of EH5 chondrite St. Mark's [7-9].

**Petrography & Mineral Chemistry:** Petrography, texture and mineral chemistry of several djerfisherite grains have been investigated using reflected light microscopy, BSE imaging, K- and Cl-mapping and quantitative EPMA analysis (University of Manchester and Open University, Cameca SX100) in ALHA 77295 ("A77", EH3) and Sahara 97096 ("S97", EH3).

Djerfisherite in A77 is present in several forms: as small 10-20  $\mu\text{m}$  sized grains dispersed in matrix, included in "fluffy" metal-troilite clasts and accreted around metal-troilite grains, discrete idiomorphic grains, as well as part of larger vein networks (here several 100  $\mu\text{m}$  long) (see Fig. 2 for examples). Similar forms were previously described for oldhamite distribution in A77 [19].

The djerfisherite grains give consistent mineral-chemical formulae, represented by:  $(\text{K},\text{Na})_{5.6-6.1}(\text{Fe},\text{Ni},\text{Cu})_{25.4-27}\text{S}_{27}\text{Cl}_{1.0-1.4}$ , consistent also with previous studies and suggestive of a homogenous djerfisherite population in A77, despite the varying grain morphologies (Fig. 2). BSE images reveal chemically unzoned and hence pristine grains [13].

S97 contains less idiomorphic djerfisherite than A77, and shows the characteristic Qingzhen “break-down” reaction into porous troilite and other phases, previously described in Qingzhen and Y-691 [12,13,15] (Fig. 3).

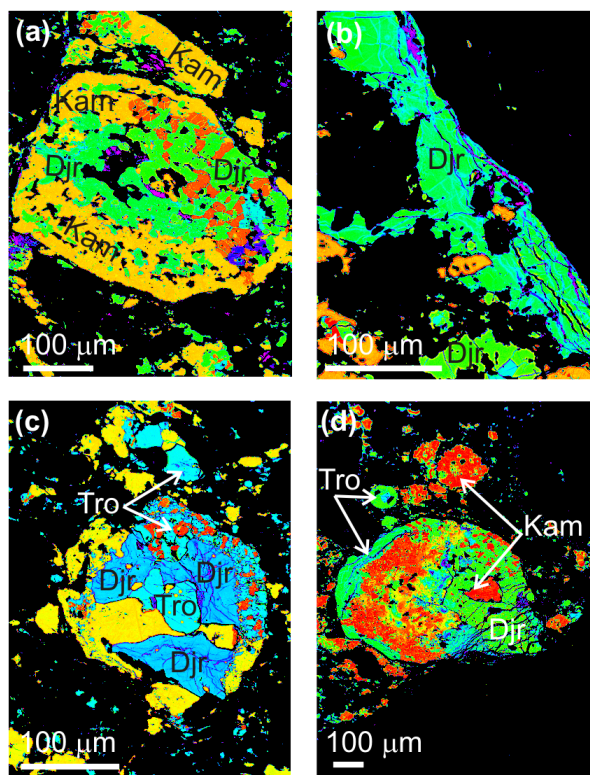


**Fig. 2** Djerfisherite (Djr) morphologies in ALHA 77295. (a) Metal-sulfide clast (Kam=Kamacite) with large, central djerfisherite grain. (b) Long, narrow djerfisherite vein dispersed along the edge of the sample. (c) Djerfisherite accreted around troilite (Tro) and included in troilite. (d) Djerfisherite accreted onto metal-troilite.

**Results & Discussion:** Idiomorphic djerfisherite in A77 is pristine, primary djerfisherite from nebula condensation, while the more common porous “broken down” djerfisherite of S97 is disturbed, due most likely to a thermal event at  $\sim 2$  Ga [20] (djerfisherite grains from Qingzhen show Ar-Ar ages between  $\sim 1.7$  and  $4.4$  Ga [21]). However, chemically, there is minimal difference between the two pristine djerfisherite popula-

tions in both meteorites. Evidence for disturbances of other sulfide phases, such as Fe-FeS eutectic melt textures, as reported in paired Sahara 97072 [22], are encountered in S97, again supporting a more complex history for this sample related to thermal metamorphic episodes. Moreover, these textural features could provide additional evidence that these EH3s originated from and evolved in different parent bodies [19].

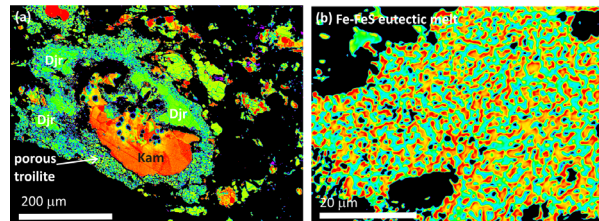


**Fig. 3** (a) Remnant of primary djerfisherite grain accreted around a large kamacite grain and surrounded by porous troilite as a result of the “Qingzhen” breakdown reaction in S97. (b) Fe-FeS eutectic melt texture observed on a 10s of micron scale in S97.

**Acknowledgements:** This work has been supported by the Leverhulme Trust and STFC. We thank M. Boyet and the NASA Meteorite Working Group for the kind allocation of the EH chondrite samples.

**References:** [1] Russell S.S. et al. 2006. in *Meteorites and the Early Solar System II*. 233-251. [2] Wadhwa M.G., Srinivasan G. and Carlson R.W. 2006. in *Meteorites and the Early Solar System II*. 715-731. [3] Krot A.N. and Bizzarro M. 2009. GCA 73: 4919-4921. [4] Gilmour J.D. 2000. Space Sci. Rev. 92: 123-132. [5] Krot A.N. et al. 2009. GCA 73: 4963-4997. [6] Min K. et al. 2003. EPSL 209: 323-336. [7] Busemann H., Baur H. and Wieler R. 2002. M&PS 37: A28. [8] Busemann H., Baur H. and Wieler R. 2002. GCA 66: A112. [9] Busemann H. et al. EPSL. in preparation. [10] Busemann H., Baur H. and Wieler R. 2000. M&PS 35: 949-973. [11] Boctor N.Z. and El Goresy A. 1986. Meteoritics 21: 336-337. [12] El Goresy A. et al. 1988. Proc. NIPR Symp. Antarct. Meteorites 1: 65-101. [13] Lin Y. and El Goresy A. 2002. M&PS 37: 577-599. [14] Podosek F.A. et al. 1990. Meteoritics 25: 399. [15] El Goresy A. 1985. Meteoritics 20: 639. [16] Woolum D.S., Brooks Cochrane R. and Joyce D. 1984. LPS XV: 935-936. [17] Fuchs L.H. 1966. Science 153: 166-167. [18] Busfield A., Turner G. and Gilmour J.D. 2008. M&PS 43: 883-897. [19] Gannoun A. et al. 2011. GCA 75: 3269-3289. [20] Torigoye N. and Shima M. 1993. Meteoritics 28: 515-527. [21] Müller N. and Jessberger E.K. 1985. LPSC XVI: 595-596. [22] Lehner S.W., Buseck P.R. and McDonough W.F. 2010. M&PS 45: 289-303.